AIMS Mathematics, 9(2): 3174–3194.
DOI: 10.3934/math.2024154
Received: 08 November 2023
Revised: 24 December 2023
Accepted: 27 December 2023
Published: 03 January 2024

http://www.aimspress.com/journal/Math

Research article

Forest model dynamics analysis and optimal control based on disease and fire interactions

Xiaoxiao Liu[1] **and Chunrui Zhang**[2,*]

[1] College of Computer and Control Engineering, Northeast Forestry University, Harbin 150040, China

[2] College of Science, Northeast Forestry University, Harbin 150040, China

* **Correspondence:** Email: math@nefu.edu.cn.

Abstract: Three models for the propagation of forest disease are revisited to include the effect of forest fires and disease spread. We study the global stability of the forest-disease model in the absence of forest fires and the spread of disease. When forest fires caused by grass cover are considered, we show that the equilibrium points are locally asymptotically stable. If both forest fires and the spread of disease exist in the second model, then Turing instability can occur. In this case, the system exhibits complex dynamic behavior. To determine the effect of fire on the forest disease model, we obtain the optimal control expression of the key parameter fire factor, and carry out sensitivity analysis. Finally, we use forest biomass data of some provinces in China from 2002 to 2018 for numerical simulation, and the results are in agreement with the theoretical analysis.

Keywords: Forest-Disease model; forest fire; stability; optimal control; sensitivity analysis
Mathematics Subject Classification: 34C23, 35K57

1. Introduction

Forest dynamics result from the interaction of natural disturbances with the demographic processes of recruitment, growth, and mortality. Forest dynamics are changing due to environmental changes, such as rising temperatures and carbon dioxide, as well as increasing natural disturbances, such as wildfires, pests, droughts, and hurricanes [1]. However, disturbance events cannot be considered in isolation because their effects are often compounded. For example, insects are a major cause of tree mortality, and the death of large numbers of trees increases the likelihood of fire [2]. Fire and disease are two disturbances that are spatially widespread. They affect ecosystem processes both in isolation and in concert [3]. Independently, fire and disease can have a major impact on ecosystems through the death of susceptible trees [4], which can lead to a cascade of changes in the ecosystem. When

fire and disease occur together, the interactions between them can either dampen the severity of one of the disturbances or amplify it [5]. = Here, we examine the impact of two natural disturbances, disease and fire, on forest development using a forest model as a case study. Our objective is to assess how these disturbances can independently or interactively affect the forest ecosystem. Recurrent fire can influence the transition from savanna to forest [6], while disease can also have a significant impact on the development of forest ecosystems. The interaction of fire and disease can have unique consequences for forest ecosystems as each disturbance can affect plant growth and mortality through different pathways. Tree survival is much higher in surface fires [7], but the growth of fire-sensitive trees can be limited by frequent burning [8]. In these ecological zones, grass is the primary fuel for surface fires. Fire intensity decreases as mature trees grow and form a closed canopy to shade out flammable grasses. Tree growth and fire have a negative feedback loop [9]. This relationship is further modified by changes in tree species composition [10]. Similar to fire, as diseases can be species or strain specific, tree species composition is important in regulating many diseases. Reduced fire frequency may make ecosystems more susceptible to disease if tree species that increase in low fire frequency environments are more susceptible to disease [11]. Simply, in the plant domain, the more densely populated a plant is, the more susceptible it is to disease [12]. This view has good empirical support in agricultural literature [13] as well as in the extensive literature exploring the Jenson Cornell effect in natural ecosystems [14]. Many plant pathogens are specific to a genus or species, such as beech bark disease, which affects several conifer species [15]. In systems with specific diseases but diverse tree communities, the colonization and growth of resistant species may compensate for the loss of susceptible species over time. For example, in forests dominated by needle oak, other fire-susceptible species (e.g. maple) are rare, which may limit their ability to replenish rapidly when fire is excluded [16]. As forest succession continues, coniferous forests are replaced by red oak and maple [17].

In [18], Adam assumes that fire only affects saplings. However, there are some trees where adults and saplings have the same sensitivity to fire. In response to this question, we improve the model, by considering the relationship between susceptible and infected trees. The number of parameters fitted has been minimized in order to facilitate the exploration of the effects of the parameters on the model. Compared with [19, 20], we consider both adults and saplings under the synergistic effect of disease and forest fire. Compared with [21, 22], tree species may diffuse in the direction of regions rich in resources, or may diffuse in areas with few competitors because of the asymmetric competition between species. The effect of spatial diffusion is considered.

The paper is structured as follows: In Section 2, we consider a forest-disease model and investigate the global asymptotic stability of the disease-free equilibrium point and the internal equilibrium point. In Section 3, we build on the Forest-Disease model by considering the disturbance of forest systems by forest fire to develop a forest-disease-fire model. The local stability of the disease-free equilibrium point as well as the internal equilibrium point is investigated. We consider the case where there is seed dispersal in an ecosystem. We add a diffusion term for susceptible and infected trees in Section 4 to explore the Turing instability of the Forest-Disease-Fire model. Numerical simulations of the Turing branch are given. Furthermore, in Section 5, to explore the effect of fire on the model, we improve the model presented in Section 3, consider the optimal control strategy for the improved model, fit the model using data from the State Forestry Administration on forest fires in each province from 2002 to 2018, and perform sensitivity analysis on key parameters in the model.

2. Global stability the of Forest-Disease model

In this section, based on [18], only considering the effect of disease, we develop a Forest-Disease model that assumes the population is divided into two compartments: $S(t)$ represents the susceptible tree, in which all individuals are susceptible to the disease and $I(t)$ represents the infected tree, in which all individuals are infected by the disease and they can transmit the disease to the healthy one. r represents the growth rate of susceptible trees, K is the environmental capacity, $\frac{\beta}{I+\alpha}SI$ represents nonlinear incidence rate, and μ is the death rate of infected trees (I). We consider the Forest-Disease model

$$\begin{cases} \frac{dS}{dt} = rS(1-\frac{S}{K}) - \frac{\beta}{I+\alpha}SI, \\ \frac{dI}{dt} = \frac{\beta}{I+\alpha}SI - \mu I. \end{cases} \tag{2.1}$$

2.1. The existence of equilibria

In this subsection, we demonstrate the existence of the equilibria. According to the biological meaning, we need all equilibria to be nonnegative. By using system (2.1), the equilibrium satisfies the equations

$$\begin{cases} rS(1-\frac{S}{K}) - \frac{\beta}{I+\alpha}SI = 0, \\ \frac{\beta}{I+\alpha}SI - \mu I = 0. \end{cases} \tag{2.2}$$

Consequently, we can immediately calculate that system (2.1) has only one disease-free equilibrium $E^0 = (S^0, 0)$, where $S^0 = K$.

Consider the internal equilibrium point $E^* = (S^*, I^*)$ of (2.1). By using the second equation of system (2.2), when $I^* \neq 0$, we get $S^* = \frac{\mu(I^*+\alpha)}{\beta}$. Substituting into the first equation of system (2.2), define $R_0 = \frac{K\beta}{\mu\alpha}$, then we obtain

$$\mu r I^2 + (2\mu r\alpha - Kr\beta + K\beta^2)I + \mu r\alpha^2 - Kr\beta\alpha = 0.$$

Because of

$$\begin{aligned} \mu r\alpha^2 - K\alpha\beta r &= r\alpha(\mu\alpha - K\beta) \\ &= r\mu\alpha^2(1 - \frac{K\beta}{\mu\alpha}) \\ &= r\mu\alpha^2(1 - R_0) \end{aligned}$$

we can observe that:

(i) If $R_0 < 1$, then there is no positive root I^*, and hence, no internal equilibrium point $E^* = (S^*, I^*)$;

(ii) If $R_0 > 1$, then there is a internal equilibrium point $E^* = (S^*, I^*)$.

2.2. Global stability of the Forest-Disease model

We present the global stability analysis corresponding to the system (2.1). Consider the disease-free equilibrium point $E^0 = (S^0, 0)$:

Theorem 1. *The disease free equilibrium point $E^0 = (S^0, 0)$ is global asymptotically stable, if $R_0 < 1$, where $R_0 = \frac{K\beta}{\mu\alpha}$.*

Proof. We prove Theorem (1) by constructing a suitable Lyapunov function, where $R_+^2 = \{(S, I)|S \geq 0, I \geq 0\}$. Consider $V(t) : R_+^2 \longrightarrow R$ such that

$$V(t) = V_1(t) + V_2(t),$$

where $V_1(t) = (S - S^0 - S^0 \ln \frac{S}{S^0}), V_2(t) = I - 0$. This particular type of Lyapunov function has been considered widely [23]. We obtain $V(t) = S - S^0 - S^0 \ln \frac{S}{S^0} + I$, and then

$$\begin{aligned}
\frac{dV}{dt} &= \frac{S - S^0}{S}[rS(1 - \frac{S}{K}) - \frac{\beta}{I + \alpha}SI] + \frac{\beta}{I + \alpha}SI - \mu I \\
&= (S - S^0)[r(1 - \frac{S}{S^0}) - \frac{\beta}{I + \alpha}I] + \frac{\beta}{I + \alpha}SI - \mu I \\
&= \frac{-r}{S^0}(S - S^0)^2 + \frac{S^0\beta}{I + \alpha}I - \mu I \\
&= \frac{-r}{S^0}(S - S^0)^2 + (\frac{S^0\beta}{I + \alpha} - \mu)I \\
&< (\frac{S^0\beta}{I + \alpha} - \mu)I.
\end{aligned}$$

Since $R_0 < 1$, $\frac{K\beta}{\alpha} - \mu < 0$. Thus, $\frac{S^0\beta}{I+\alpha} \leq \frac{K\beta}{\alpha}$ and we conclude that $\frac{dV}{dt} < 0$ along all the trajectories in R_+^2 and $\frac{dV}{dt} = 0$ at $E^0 = (S^0, 0)$. Therefore, by LaSalle's theorem, E^0 is globally asymptotically stable. □

Next, we present the global stability analysis of the internal equilibrium $E^* = (S^*, I^*)$.

Theorem 2. *The internal equilibrium $E^* = (S^*, I^*)$ exists and is globally asymptotically stable if $R_0 > 1$ and $\frac{\beta I^*}{2\alpha^2} < \min\{\frac{r}{K}, \frac{S^*\beta}{2\alpha^2}\}$.*

Proof. We consider the following Lyapunov function:

$$V = S - S^* - S^* \ln \frac{S}{S^*} + I - I^* - I^* \ln \frac{I}{I^*}.$$

The time derivative of V along the solution of system (2.1) is:

$$\begin{aligned}
\frac{dV}{dt} &= \frac{S - S^*}{S}[rS(1 - \frac{S}{K}) - \frac{\beta}{I + \alpha}SI] + \frac{I - I^*}{I}(\frac{IS\beta}{\alpha + I} - \mu I) \\
&= (S - S^*)[r(1 - \frac{S}{K}) - \frac{I\beta}{I + \alpha}] + (I - I^*)(\frac{\beta S}{I + \alpha} - \mu) \\
&\leq -\frac{r}{K}(S - S^*)^2 + \beta(S - S^*)(\frac{I^*}{I^* + \alpha} - \frac{I}{I + \alpha}) + \beta(I - I^*)(\frac{S}{I + \alpha} - \frac{S^*}{I^* + \alpha}) \\
&\leq -\frac{r}{K}(S - S^*)^2 + \beta\frac{(I - I^*)(SI^* - S^*I)}{(I + \alpha)(I^* + \alpha)} \\
&\leq (S - S^*)^2(\frac{\beta I^*}{2\alpha^2} - \frac{r}{K}) + (I - I^*)(\frac{\beta I^*}{2\alpha^2} - \frac{S^*\beta}{2\alpha^2}).
\end{aligned}$$

We conclude that $\frac{dV}{dt} < 0$ along all the trajectories in R_+^2 and $\frac{dV}{dt} = 0$ at $E^* = (S^*, I^*)$. Therefore, by LaSalle's theorem, E^* is globally asymptotically stable. □

3. Fire based Forest-Disease model

On the basis of system (2.1), we model the fire effect as a factor that kills sensitive trees, with fire-driven mortality as a function of potential intensity, controlled by grass cover, which is implicitly modeled as a decreasing function of the number of sensitive trees (S) in the measurement area $\frac{1}{\omega S+1}$. Ecologically, this is because trees shade grassland, but shading is a nonlinear saturation function of tree abundance. Then, both frequency and intensity are related to mortality through the parameter σ. The functional form of the tree-grass relationship is determined empirically by nonlinear least squares fitting and model selection [18]. We model how grass cover changes the fire frequency effect by adding a term σ, resulting in a single parameter that incorporates both intensity and frequency into a severity indicator. We consider the Forest-Disease-Fire model as follows:

$$\begin{cases} \frac{dS}{dt} = rS(1-\frac{S}{K}) - \frac{\beta}{I+\alpha}SI - \sigma\frac{S}{\omega S+1}, \\ \frac{dI}{dt} = \frac{\beta}{I+\alpha}SI - \mu I. \end{cases} \tag{3.1}$$

3.1. The existence of equilibria

By using system (3.1), the equilibrium satisfies the equations

$$\begin{cases} rS(1-\frac{S}{K}) - \frac{\beta}{I+\alpha}SI - \sigma\frac{S}{\omega S+1} = 0, \\ \frac{\beta}{I+\alpha}SI - \mu I = 0. \end{cases}$$

Since $I = 0$, we substitute into the first equation $rS(1-\frac{S}{K}) - \sigma\frac{S}{\omega S+1} = 0$. Then,

$$S^1 = \frac{r(K\omega-1) + \sqrt{r^2(1-K\omega)^2 + 4rK\omega(r-\sigma)}}{2r\omega}.$$

When $K\omega < 1$, system (3.1) has only one disease-free equilibrium $E^1 = (S^1, 0)$, and thus, the disease-free equilibrium $E^1 = (S^1, 0)$ exists.

We now consider the internal equilibrium point $E^* = (S^*, I^*)$ of (3.1):

Lemma 1. *The internal equilibrium E_f^* exists if $R_2 = \frac{S_f^*\beta}{\alpha\mu} > 1$ and $S_1 < \frac{\mu\alpha}{\beta} < S_f^*$.*

Proof. The internal equilibrium $E_f^* = (S_f^*, I_f^*)$ can be determind by

$$\begin{cases} I_f^* = \frac{\beta}{\mu}S_f^* - \alpha, \\ a_0 S_f^{*3} + a_1 S_f^{*2} + a_2 S_f^* + a_3 = 0, \end{cases}$$

where $a_0 = r\omega$, $a_1 = r - K\omega r + K\omega\beta$, $a_2 = K(\beta - \alpha\mu\omega - r + \alpha)$, $a_3 = -K\alpha\mu$.

Define a function $f(S) = a_0S^3 + a_1S^2 + a_2S + a_3$. Then, S_f^* is a solution of $f(S) = 0$. Since $a_0 > 0$, $a_3 < 0$, $f(S)$ has at least one positive solution S_f^*.

Since $I_f^* = \frac{\beta}{\mu}S_f^* - \alpha > 0$, then we need $S_f^* > \frac{\mu\alpha}{\beta}$. Here, the basic reproduction number $R_2 = \frac{S_f^*\beta}{\alpha\mu}$. $f'(S) = 3a_0S^2 + 2a_1S + a_2$, and thus, S_1 and S_2 are solutions of $f'(S) = 0$. If $K\omega > 1$, then

$0 < S_1 < S_f^* < S_2$, see Figure 1. According to this, if $K\omega > 1$, $r < \sigma$, and $\frac{\alpha\mu}{\beta} > \frac{K\omega-1}{\omega}$ hold, then

$$\begin{aligned} f(\frac{\alpha\mu}{\beta}) &= \frac{\alpha\mu}{\beta^3}(-Kr\beta^2 + r\alpha\beta\mu + K\sigma\beta^2 - Kr\alpha\beta\mu\omega + r\alpha^2\mu^2\omega) \\ &> \frac{\alpha\mu}{\beta^3}(-Kr\beta^2 + r\alpha\beta\mu + K\sigma\beta^2 - Kr\alpha\beta\mu\omega + r\alpha\mu(K\omega\beta - \beta)) \\ &= \frac{\alpha\mu}{\beta^3}(K\beta^2(\sigma - r)) > 0. \end{aligned}$$

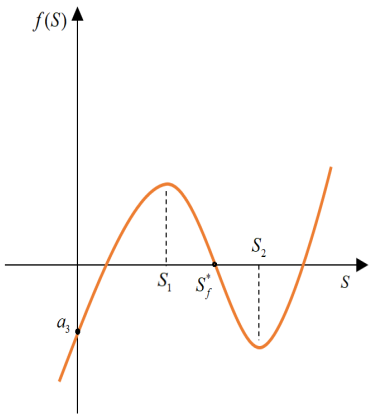

Figure 1. Graph of the function $f(S)$.

Since $S_1 < \frac{\mu\alpha}{\beta} < S_f^*$, the internal equilibrium E_f^* exists. □

3.2. Local stability of the fire based Forest-Disease model

Next we will perform a local stability analysis on system (3.1). For $E^1 = (S^1, 0)$, the Jacobian matrix is

$$J|_{E^1(S^1,0)} = \begin{pmatrix} -\frac{rS^1}{K} + \frac{\sigma\omega S^1}{(1+S^1\omega)^2} & -\frac{S^1\beta}{\alpha} \\ 0 & \frac{S^1\beta}{\alpha} - \mu, \end{pmatrix}$$

and

$$\triangle = \lambda^2 + (\frac{rS^1}{K} - \frac{\sigma\omega S^1}{(1+S^1\omega)^2} - \frac{S^1\beta}{\alpha} + \mu)\lambda + S^1(S^1\beta - \alpha\mu)(\frac{-r}{K\alpha} + \frac{\sigma\omega}{\alpha(1+S^1\omega)^2}).$$

Here, the basic reproduction number $R_1 = \frac{S^1\beta}{\alpha\mu} < 1$ is defined.

Theorem 3. *The disease-free equilibrium $E^1 = (S^1, 0)$ is locally asymptotically stable if $R_1 < 1$, $K\omega < 1$, and $r > \sigma$.*

Proof. Clearly, if $K\omega < 1$ and $r > \sigma$ hold, then

$$-\frac{r}{K} + \frac{\sigma\omega}{(1+S^1\omega)^2} < \frac{-r}{K} + \sigma\omega = \frac{-r + \sigma\omega K}{K} < \frac{-r + r\omega K}{K} = \frac{r(\omega K - 1)}{K} < 0.$$

According to this, then

$$\lambda_1 + \lambda_2 = -\frac{rS^1}{K} + \frac{\sigma\omega S^1}{(1+S^1\omega)^2} + \frac{S^1\beta}{\alpha} - \mu < 0,$$

and

$$\lambda_1\lambda_2 = S^1(S^1\beta - \alpha\mu)(\frac{-r}{K\alpha} + \frac{\sigma\omega}{\alpha(1+S^1\omega)^2}) > 0.$$

We conclude that when the basic reproduction number $R_1 < 1$, $K\omega < 1$, and $r > \sigma$, E^1 is locally asymptotically stable. □

Theorem 4. *If $K\omega > 1$, $r < \sigma < K\omega r$, and $\frac{\alpha\mu}{\beta} > \frac{K\omega-1}{\omega}$ hold, $E_f^* = (S_f^*, I_f^*)$ is locally asymptotically stable.*

Proof.

$$J|_{E_f^*(S_f^*,I_f^*)} = \begin{pmatrix} -\frac{rS_f^*}{K} + \frac{S_f^*\sigma\omega}{(1+S_f^*\omega)^2} & -\frac{S_f^*\beta\alpha}{(I_f^*+\alpha)^2} \\ \frac{\beta I_f^*}{I_f^*+\alpha} & \frac{S_f^*\beta\alpha}{(I_f^*+\alpha)^2} - \mu \end{pmatrix}$$

and

$$\begin{aligned} \triangle = \lambda^2 &+ \left(\frac{rS_f^*}{K} - \frac{S_f^*\beta\alpha}{(\alpha+I_f^*)^2} - \frac{\sigma\omega S_f^*}{(1+S_f^*\omega)^2} + \mu\right)\lambda \\ &+ \mu\left(\frac{\alpha\mu\left(S_f^*\beta - \alpha\mu\right)}{S_f^{*2}\beta} + (1 - \frac{\alpha\mu}{S_f^*\beta}) \cdot \frac{S_f^*(-K\sigma\omega + r(1+S_f^*\omega)^2)}{K(1+S_f^*\omega)^2}\right). \end{aligned}$$

Clearly,

$$\begin{aligned} \lambda_1 + \lambda_2 &= -\frac{rS_f^*}{K} + \frac{\sigma\omega S_f^*}{(1+S_f^*\omega)^2} + \frac{S_f^*\beta\alpha}{(\alpha+I_f^*)^2} - \mu = -\frac{rS_f^*}{K} - \mu + \frac{\alpha\mu^2}{S_f^*\beta} + \frac{\sigma\omega S_f^*}{(1+S_f^*\omega)^2} \\ &< -\frac{rS_f^*}{K} - \mu + \mu + \frac{\sigma S_f^*}{K^2\omega} = \frac{S_f^*(\sigma - K\omega r)}{K^2\omega} < 0 \end{aligned}$$

and

$$\begin{aligned} \lambda_1\lambda_2 &= \mu\left(\frac{\alpha\mu\left(S_f^*\beta - \alpha\mu\right)}{S_f^{*2}\beta} + (1 - \frac{\alpha\mu}{S_f^*\beta}) \cdot \frac{S_f^*(-K\sigma\omega + r(1+S_f^*\omega)^2)}{K(1+S_f^*\omega)^2}\right) \\ &> \mu\left(\frac{\alpha\mu\left(S_f^*\beta - \alpha\mu\right)}{S_f^{*2}\beta} + (1 - \frac{\alpha\mu}{S_f^*\beta}) \cdot \frac{S_f^*K\omega(-\sigma + K\omega r)}{K(1+S_f^*\omega)^2}\right) > 0. \end{aligned}$$

□

In order to verify the asymptotic stability of the system, numerical simulation is performed on the model (3.1). Using the parameter values $r = 0.62117, K = 85, \alpha = 37, \beta = 2, \sigma = 0.60137, \omega = 0.9$, and $\mu = 0.6$, we obtain positive equilibrium points ($S_f^* = 14.5313, I_f^* = 11.4376$). These parameters

are selected following reference [18]. These parameter values satisfy the conditions of the theorem analyzed above. The above analysis shows that the system is asymptotically stable, as shown in Figure 2. The figure on the left shows the S_f^* endemic state for fire, and the figure on the right shows the I_f^* endemic state for fire.

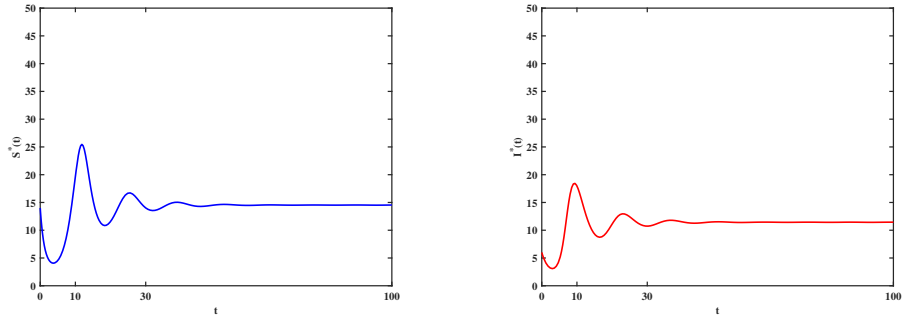

(a) (b)

Figure 2. The numerical simulations of system (3.1). (**a**): component S_f^* (Locally asymptotically stable); (**b**): component I_f^* (Locally asymptotically stable).

Remark 1. *In Section 2, we analyzed the global stability of the no-fire model. If* $R_0 < 1$, $E^0 = (S^0, 0)$ *is global asymptotically stable, and if* $R_0 > 1$, *the internal equilibrium* $E^* = (S^*, I^*)$ *exists and is globally asymptotically stable, and we obtain the basic reproduction number* $R_0 = \frac{K\beta}{\mu\alpha}$. *In Section 3, we considered the local stability of the model under fire disturbance. If* $R_1 = \frac{S^1\beta}{\alpha\mu} < 1$, E^1 *is locally asymptotically stable. If* $R_2 = \frac{S_f^*\beta}{\alpha\mu} > 1$, *the internal equilibrium* E_f^* *exists and is locally asymptotically stable.*

4. Fire and diffusion based Forest-Disease model

Species distributions are both static and dynamic, and as forests evolve, communities maintain biodiversity through diffusion. It is therefore of practical importance to study the diffusion of populations of forest tree species. To get closer to the evolutionary process of biodynamic systems, the spatial evolution of the model needs to be further considered. Taking into account the reproduction of tree species, we add diffusion terms for susceptible and infected trees. For model (3.1) under the coupling of the fire, tree species may diffuse in the direction of regions rich in resources, or may diffuse in areas with few competitors because of the asymmetric competition between species, or may diffuse with the influence of external environmental factors such as water flow. Based on the above complex ecological process, it is reasonable to describe the relationship between susceptible and infected trees by using the reaction-diffusion equation.

4.1. Linear stability analysis

Consider the diffusion equations

$$\begin{cases} \frac{\partial S}{\partial t} = D_S \Delta S + rS(1 - \frac{S}{K}) - \frac{\sigma S}{\omega S + 1} - \frac{\beta S I}{I + \alpha}, \\ \frac{\partial I}{\partial t} = D_I \Delta I + \frac{\beta S I}{I + \alpha} - \mu I. \end{cases} \tag{4.1}$$

In this section, D_S and D_I represent diffusion coefficients, and $\Delta = \partial^2/\partial S^2 + \partial^2/\partial I^2$ is the Laplace operator in space. We perform a linear stability analysis [24] of system (4.1). To simplify the discussion of system (4.1), we transform the positive equilibrium point (S^*, I^*) into $(0, 0)$ by the means of transformation $(S, I) = (S^* + \widetilde{S}, I^* + \widetilde{I})$. Then, we can obtain the linearized system as follows:

$$\begin{cases} \frac{\partial \widetilde{S}}{\partial t} = d_1 \Delta \widetilde{S} + [r(1 - \frac{2S^*}{K}) - \frac{\sigma}{(1+\omega S^*)^2} - \frac{\beta I^*}{I^*+\alpha}]\widetilde{S} - \frac{S^*\alpha\beta}{(I^*+\alpha)^2}\widetilde{I}, \\ \frac{\partial \widetilde{I}}{\partial t} = d_2 \Delta \widetilde{I} + \frac{\beta I^*}{I^*+\alpha}\widetilde{S} + (\frac{S^*\alpha\beta}{(I^*+\alpha)^2} - \mu)\widetilde{I}. \end{cases} \tag{4.2}$$

We denote $p_1 = r(1 - \frac{2S^*}{K}) - \frac{\sigma}{(1+\omega S^*)^2} - \frac{\beta I^*}{I^*+\alpha}, q_1 = -\frac{S^*\alpha\beta}{(I^*+\alpha)^2}, p_2 = \frac{\beta I^*}{I^*+\alpha}, q_2 = \frac{S^*\alpha\beta}{(I^*+\alpha)^2} - \mu$.
Let $d_1 = \varepsilon d, d_2 = d$, then we can get $\varepsilon = \frac{d_1}{d_2} > 0$. We rewrite Eq (4.2) as

$$\begin{cases} \frac{\partial \widetilde{S}}{\partial t} = \varepsilon d \triangle \widetilde{S} + p_1 \widetilde{S} + q_1 \widetilde{I}, \\ \frac{\partial \widetilde{I}}{\partial t} = d \triangle \widetilde{S} + p_2 \widetilde{S} + q_2 \widetilde{I}. \end{cases} \tag{4.3}$$

We can then obtain the Jacobian matrix

$$J = \begin{pmatrix} p_1 - \varepsilon d k^2 \pi^2 & q_1 \\ p_2 & q_2 - k^2 \pi^2 d \end{pmatrix}.$$

Then, the characteristic equation of J is

$$D_k(\lambda, \varepsilon) = \lambda^2 - TR_k \lambda + DET_k = 0,$$

with

$$\begin{aligned} TR_k &= -(\varepsilon + 1) d k^2 \pi^2 + p_1 + q_2, \\ DET_k &= \varepsilon d^2 k^4 \pi^4 - d k^2 \pi^2 (p_1 + q_2 \varepsilon) + p_1 q_2 - p_2 q_1. \end{aligned}$$

Now, we assume that

$$B_0 \begin{cases} p_1 + q_2 < 0, \\ p_1 q_2 - p_2 q_1 > 0. \end{cases}$$

Lemma 2. *Suppose that* (B_0) *holds. Then, the ordinary differential equation system corresponding to system (4.1) is locally asymptotically stable at the positive equilibrium point* (S^*, I^*).

Proof. We can get the characteristic equation of the ordinary differential equation system when the diffusion term is not added. That is,

$$D_0(\lambda, \varepsilon) = \lambda^2 - TR_0 \lambda + DET_0 = 0$$

with

$$\begin{aligned} TR_0 &= p_1 + q_2, \\ DET_0 &= p_1 q_2 - p_2 q_1. \end{aligned}$$

Both roots of $D_0(\lambda, \varepsilon) = 0$ have negative real parts when $TR_0 < 0$ and $DET_0 > 0$. Therefore, system (4.1) is asymptotically stable at the positive equilibrium point (S^*, I^*). Hence, the lemma is proved. □

4.2. Analysis of Turing instability

Now we consider the existence conditions for Turing instability.

Assume that

(B_1) $0 < \varepsilon < \varepsilon_1$, where $\varepsilon_1 \triangleq \frac{-2p_2q_1+p_1q_2-2\sqrt{p_2^2q_1^2-p_1p_2q_1q_2}}{q_2^2}$.

(B_2) $0 < \varepsilon < \varepsilon_2(d)$, where $\varepsilon_2(d) \triangleq \frac{p_1}{d\pi^2-q_2}$. $\varepsilon = \varepsilon(d)$ decreases monotonically in d and intersects with $\varepsilon = \varepsilon_1$ at the point $d = d_0$. We take $\varepsilon_B(d) = \min\{\varepsilon_1, \varepsilon_2(d)\}$, then

$$\varepsilon_B(d) = \begin{cases} \varepsilon_1, 0 < d \leq d_0 \\ \varepsilon_2(d), d > d_0. \end{cases}$$

Proof. Let $x = dk^2\pi^2 > 0$, then we rewrite DET_k as

$$DET_k = \varepsilon x^2 - (p_1 + q_2\varepsilon)x + p_1q_2 - p_2q_1.$$

Then, we get that the symmetry axis is $x = \frac{p_1+q_2\varepsilon}{2\varepsilon}$, and at this time DET_k can be taken to a minimum. That is,

$$DET_{k_{min}} = p_1q_2 - p_2q_1 - \frac{(p_1 + q_2\varepsilon)^2}{4\varepsilon}.$$

Since $x > 0$, we have $p_1 + q_2\varepsilon > 0$. If we want $DET_{k_{min}} < 0$ with the condition $p_1 + q_2\varepsilon > 0$, we must satisfy $p_1q_2 - p_2q_1 - \frac{(p_1+q_2\varepsilon)^2}{4\varepsilon} < 0$. We can obtain

$$0 < \varepsilon < \frac{-2p_2q_1 + p_1q_2 - 2\sqrt{p_2^2q_1^2 - p_1p_2q_1q_2}}{q_2^2},$$

when

$$p_1 > 0, q_1 < 0, q_2 < -p_1, p_2 > \frac{p_1q_2}{q_1}.$$

Let $\varepsilon_1 = \frac{-2p_2q_1+p_1q_2-2\sqrt{p_2^2q_1^2-p_1p_2q_1q_2}}{q_2^2}$. Then, when $0 < \varepsilon < \varepsilon_1$, it ensures that the symmetry axis is greater than 0, and Turing instability occurs at (S^*, I^*).

Next, we take the value of x between the symmetry axis and the right root of DET_k. Then, $\frac{p_1+q_2\varepsilon}{2\varepsilon} \leqslant x \leqslant \frac{p_1+q_2\varepsilon+\sqrt{\triangle}}{2\varepsilon}$. k can be taken to the minimum when x takes a value on the symmetry axis, and we get

$$k_{min}^2 = \frac{p_1 + q_2\varepsilon}{2\varepsilon} \cdot \frac{1}{d\pi^2} = \frac{1}{2d} \cdot \frac{p_1 + q_2\varepsilon}{\varepsilon\pi^2},$$

and

$$k_{min} = \sqrt{\frac{1}{2} \cdot \frac{p_1 + q_2\varepsilon}{d\varepsilon\pi^2}}.$$

By making sure that $\sqrt{\frac{1}{2} \cdot \frac{p_1+q_2\varepsilon}{d\varepsilon\pi^2}} > \sqrt{\frac{1}{2}}$, we can obtain $0 < \varepsilon < \frac{p_1}{d\pi^2-q_2}$. When $p_1 > 0, q_1 < 0, q_2 < -p_1, p_2 > \frac{p_1q_2}{q_1}$, let $\varepsilon_2(d) = \frac{p_1}{d\pi^2-q_2}$, and we can find that $\varepsilon = \varepsilon_2(d)$ decreases monotonically in d and intersects with $\varepsilon = \varepsilon_1$ at the point $d = d_0$, where

$$d_0 = \frac{-2p_2q_1q_2 + 2p_1q_2^2 - 2q_2\sqrt{p_1q_1(p_2q_1 - p_1q_2)}}{\pi^2(-2p_2q_1 + p_1q_2 - 2q_2\sqrt{p_1q_1(p_2q_1 - p_1q_2)})}.$$

□

The next step is to determine the bounds of the Turing instability. We denote

$$\varepsilon_*(k,d) = \frac{dk^2\pi^2 p_1 + p_2q_1 - p_1q_2}{dk^2\pi^2(dk^2\pi^2 - q_2)}, d > d_k,$$

where $d_k = \frac{p_1q_2 - p_2q_1}{k^2\pi^2 p_1}$. Then, $DET_k = 0$, when $\varepsilon = \varepsilon_*(k,d)$. That is,

$$DET_k = 0 \Leftrightarrow \varepsilon_*(k,d) = \frac{dk^2\pi^2 p_1 + p_2q_1 - p_1q_2}{dk^2\pi^2(dk^2\pi^2 - q_2)}.$$

Then

$$\frac{d\varepsilon_*}{dx} = \frac{-p_1x^2 - 2p_1q_1x + 2p_1q_2x + p_2q_1q_2 - p_1q_2^2}{x^2(x-q_2)^2},$$

and we can get

$$d = \frac{-p_2q_1 + p_1q_2 + \sqrt{p_2^2q_1^2 - p_1p_2q_1q_2}}{p_1} \cdot \frac{1}{k^2\pi^2}.$$

Set $d_M = \frac{-p_2q_1 + p_1q_2 + \sqrt{p_2^2q_1^2 - p_1p_2q_1q_2}}{p_1} \cdot \frac{1}{k^2\pi^2}$, then $\frac{d\varepsilon_*}{dx} = 0$, when $d = d_M$. At this time, $\varepsilon_*(k,d)$ reaches the maximum value ε_1.

Lemma 3. *Suppose that (B_0) holds, function $\varepsilon = \varepsilon_*(k,d)$ has the following properties: (1) When $0 < d < d_M(k)$, $\varepsilon_*(k,d)$ increases monotonically, and when $d > d_M(k)$, $\varepsilon_*(k,d)$ decreases monotonically. (2) As for $k_i < k_{i+1}, k_i \in N, i = 1,2,3,\cdots$, there is only one root $d_{k1,k2} \in (d_M(k_2), d_M(k_1))$ satisfying $\varepsilon_*(k_1,d) = \varepsilon_*(k_2,d)$ for $d > 0$. Furthermore,*

$$\varepsilon_* = \varepsilon_*(d) = \varepsilon_*(k,d), k \in (d_{k_{i+1},i+2}, k_{i,i+i}), k_i \in N, i = 1,2,3,\cdots.$$

In Figure 3, we characterize a graph of functions $\varepsilon = \varepsilon_1, \varepsilon = \varepsilon_2(d)$, and $\varepsilon = \varepsilon_*(k,d), d > 0, k = 1,2,3,\cdots$. The value of parameters are selected following reference [18], and the value of p_1, q_1, p_2, q_2 are calculated from the model (4.2). In Figure 4, we present a graph of the Turing bifurcation line $\varepsilon = \varepsilon_*(k,d), d > 0$.

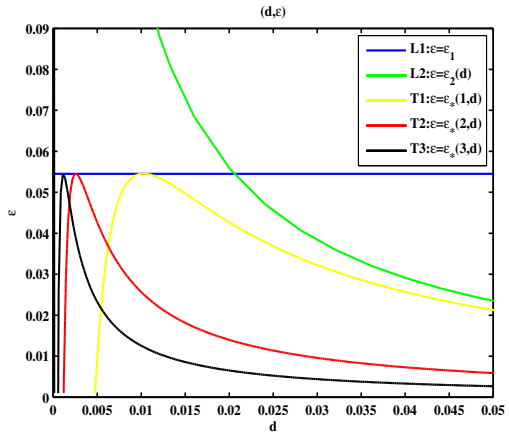

Figure 3. The figure of functions $\varepsilon = \varepsilon_1, \varepsilon = \varepsilon_2(d)$, and $\varepsilon = \varepsilon_*(k,d), d > 0, k = 1,2,3$ in (d,ε) plane. $r = 0.721, K = 90, \sigma = 0.601, \alpha = 37.854, \beta = 0.318, \omega = 0.055, \mu = 0.02$. $(S^*, I^*) \approx (17.252, 236.374)$, $p_1 = 0.0120, q_1 = -0.0028, p_2 = 0.2740, q_2 = -0.0172$.

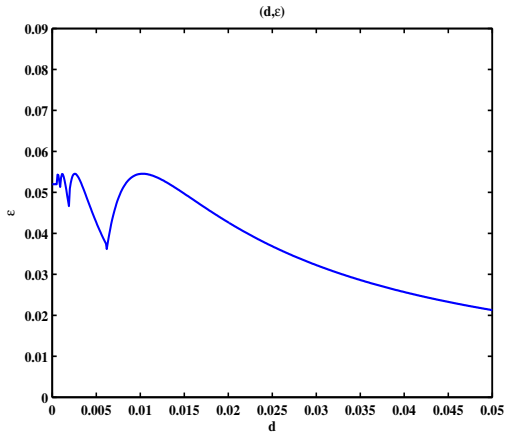

Figure 4. The Turing bifurcation line $\varepsilon = \varepsilon_*(d)(d > 0)$.

4.3. Numerical simulations of Turing bifurcation

Let $D_S = 0.03, D_I = 0.41, r = 0.721, K = 90, \sigma = 0.601, \alpha = 37.8537234, \beta = 0.318, \omega = 0.055$, and $\mu = 0.02$. We then obtain the positive equilibrium of system (4.2), $(S^*, I^*) = (17.252, 236.374)$. Through (B_1), (B_2), we obtain $\varepsilon_1 = 0.0545$,

$$\varepsilon_B(d) = \begin{cases} 0.0545, 0 < d \leq 0.0205, \\ \frac{0.0120}{d\pi^2+0.0172}, d > 0.0205, \end{cases}$$

and

$$\varepsilon_*(k, d) = \frac{0.012dk^2\pi^2 - 0.0005608}{dk^2\pi^2(dk^2\pi^2 + 0.0172)}, d > d_k.$$

Then, we can find $\varepsilon > \varepsilon_*(d)$, so system (4.2) is asymptotically stable at (S^*, I^*), see Figure 5. By setting $k = 1$, we obtain $d_{0,1} = +\infty$ and $d_{1,2} = 0.0250246$, and select $d = d_1 = 0.12 \in (d_{0,1}, d_{1,2})$; thus, $\varepsilon_* = \varepsilon_*(1, 0.12) = 0.0011360854$. System (4.2) with $d = 0.12$ undergoes a Turing bifurcation near equilibrium $(17.252, 236.374)$ at $\varepsilon = 0.0011360854$. Figure 6 shows that system (4.2) has a Turing instability near the equilibrium point $(17.252, 236.374)$ at this time.

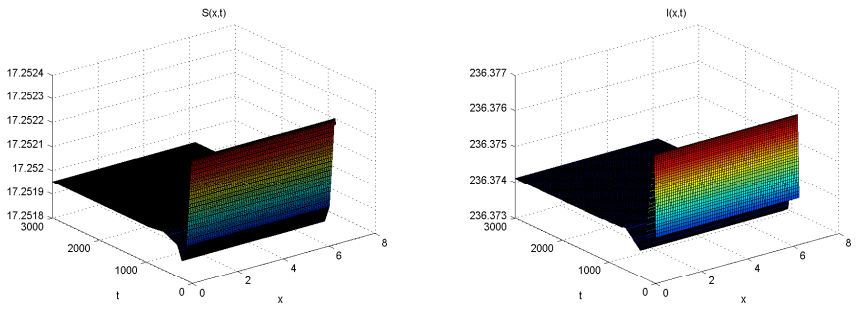

(a) (b)

Figure 5. The numerical simulations of system (4.2). (a): component S (Locally asymptotically stable); (b): component I (Locally asymptotically stable).

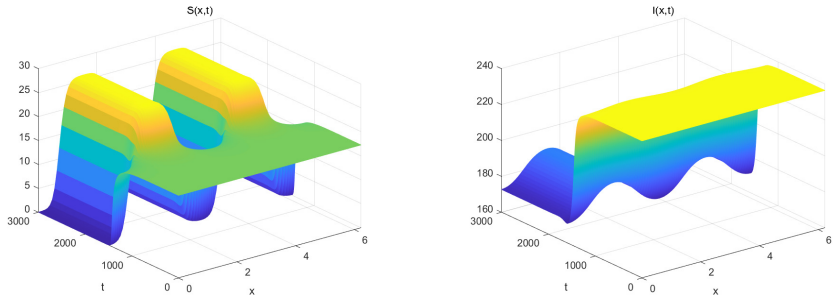

(a) (b)

Figure 6. The numerical simulations of system (4.2) with $\varepsilon = 0.00111725$ and the initial condition at $(17.252, 236.374)$. (a): component S (Turing instability); (b): component I (Turing instability).

5. Optimal control strategy and sensitivity analysis

To better describe the effect of fire on model (3.1), we rewrite the model as

$$\begin{cases} \frac{dS}{dt} = rS(1-\frac{S}{K}) - \frac{\beta}{I+\alpha}SI - \sigma\frac{S}{\omega S+1}, \\ \frac{dI}{dt} = \frac{\beta}{I+\alpha}SI - \mu_1 I - \sigma I, \end{cases} \tag{5.1}$$

where $\mu_1 = \mu - \sigma$ is the natural mortality rate of diseased trees, and σI stands for diseased trees which died due to fire. In forest ecosystems, fire is a potential threat to tree growth, and fire can directly affect forest insect populations and abundance. Therefore, one of the most important tools to reduce fire damage and insect outbreaks is to control fire intensity. Finding the right frequency of fire is an optimization problem such that damage to trees is reduced and beetles can be eliminated. In this section, we analyze the influence of key parameters on the model and use forest area data coupled with the model to construct a more complex forest model in both a fire and insect infested environment in order to gain insight into the effects of the synergistic effects of both fire and pest natural disturbances on the model.

5.1. Optimal control strategy

Optimization strategies have always played a key role in optimizing ecosystem structure and resource use patterns [25] and in identifying appropriate management actions to ensure that the overall benefits of the system are maximized. In the following sections, we will discuss optimal fire frequency management strategies. The σ in the system is set to be the time-dependent function $\sigma(t)$, describing the time-varying fire intensity, and there exists $\overline{\sigma}$ such that $0 \le \sigma(t) \le \overline{\sigma}$. Within the fixed time $[0, T]$ with $T > 0$, the constraint set reads

$$U = \{\sigma(t) | 0 \le \sigma(t) \le \overline{\sigma}, 0 \le t \le T, \sigma(t) \textit{ is Lebesgue measurable}\}. \tag{5.2}$$

Since the parameter $\sigma(t)$ is related to mortality, we aim to minimize the frequency and intensity of fire. The quadratic optimal objective function is

$$J(\sigma) = \int_0^T (\frac{1}{2}I^2(t) + \frac{1}{2}\sigma^2(t))dt,$$

with $I(0) = I_0, \sigma(0) = \sigma_0$. The optimal control problem is rewritten

$$J^*(\sigma^*(\cdot)(t)) = \min_{\sigma(t)\in U} J(\sigma(t)), \tag{5.3}$$

where the minimization of $J(\sigma(t))$ is subject to (5.1) and $\sigma \in U$ with U from (5.2).

Using the method in [26], we check the existence of optimal control $\sigma(t)$ by satisfying H5–H8 in the following:

H5: The set of state and control variables are nonempty;

H6: The set U of the control variables is closed and convex;

H7: The right side of each equation in the control problem is continuous with a bounded sum of controls and states above. This can be written as a linear function of U with coefficients that depend on time and state [27];

H8: There exists constants $\sigma > 0$ such that the integrand $L(\sigma(t))$ of the objective functional J is convex and satisfied.

We have $L(\sigma(t)) = \frac{1}{2}(I^2(t) + \sigma^2(t))$.

Theorem 5. *For the optimal control problems (5.2) and (5.3), there exists an optimal control σ^* such that $J^*(\sigma^*(\cdot)(t)) = \min_{\sigma(t)\in U} J(\sigma(t))$.*

To obtain the minimum value of (5.3), we give the Hamiltonian function:

$$H = \frac{1}{2}(I^2 + \sigma^2) + \lambda_1[rS(1 - \frac{S}{K}) - \frac{\beta}{I+\alpha}SI - \sigma\frac{S}{\omega S + 1}] + \lambda_2[\frac{\beta}{I+\alpha}SI - \mu_1 I - \sigma I],$$

where λ_1, λ_2 are adjoint variables satisfying the following adjoint equations:

$$\begin{cases} \frac{\partial H}{\partial \lambda_1}|_{(\sigma^*,\lambda_1,\lambda_2,t)} = -\dot{\lambda}_1, \lambda_1(T) = 0, \\ \frac{\partial H}{\partial \lambda_2}|_{(\sigma^*,\lambda_1,\lambda_2,t)} = -\dot{\lambda}_2, \lambda_2(T) = 0. \end{cases}$$

The optimality conditions are given by

$$\frac{\partial H}{\partial \sigma}|_{(\sigma^*,\lambda_1,\lambda_2,t)} = 0.$$

Theorem 6. *The optimal control of (5.2) and (5.3) is given by*

$$\sigma^* = \min\{\overline{\sigma}, \max\{\lambda_1\frac{S}{\omega S + 1} + \lambda_2 I, 0\}\}, \tag{5.4}$$

where λ_1, λ_2 are adjoint variables satisfying the second and third Maximum Principle condition.

Proof. According to Pontryagin's Maximum Principle, finding the optimal control of (5.2) and (5.3) is equivalent to minimizing the Hamiltonian function H defined previously.

$\frac{\partial H}{\partial \sigma}|_{(\sigma^*,\lambda_1,\lambda_2,t)} = 0$ gives $\sigma^* - \lambda_1\frac{S}{\omega S+1} - \lambda_2 I = 0$, where the adjoint variables are satisfied. Furthermore,

$$\dot{\lambda}_1 = -\frac{\partial H}{\partial S}|_{(\sigma^*,\lambda_1,\lambda_2,t)} = \lambda_1(-r + \frac{2rS}{K} + \frac{I\beta}{I+\alpha} + \frac{\sigma}{(1+S\omega)^2}) - \frac{\lambda_2 I\beta}{I+\alpha}.$$
$$\dot{\lambda}_2 = -\frac{\partial H}{\partial I}|_{(\sigma^*,\lambda_1,\lambda_2,t)} = -I + \lambda_1(\frac{S\beta}{I+\alpha} - \frac{IS\beta}{(I+\alpha)^2}) + \lambda_2(\frac{IS\beta}{(I+\alpha)^2} - \frac{S\beta}{I+\alpha} - \mu - \sigma),$$

and the transversality conditions are $\lambda_1(T) = 0, \lambda_2(T) = 0$.

Moreover, since $\sigma^* \in U$, using the lower and upper bounds of $\overline{\sigma}(t)$, the optimal $\sigma^*(t)$ can be characterized by (5.4). The curves of $\sigma^*(t)$, $S^*(t)$, and $I^*(t)$ with time for different ω are given in Figure 7. □

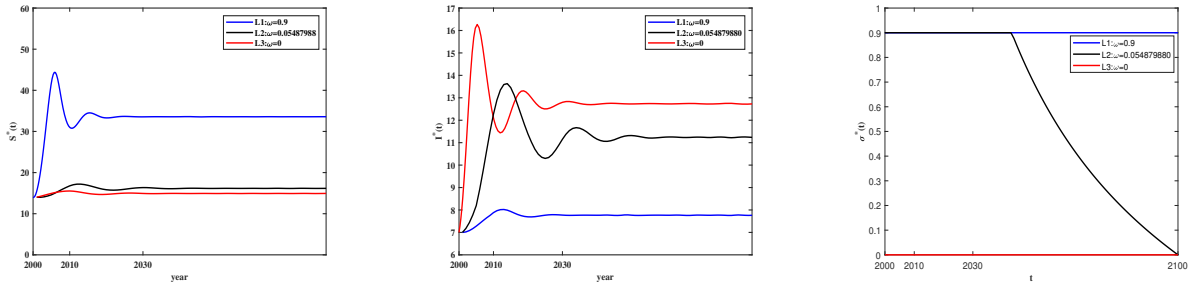

(a) (b) (c)

Figure 7. The optimal control $\sigma^*(t)$, and the corresponding $S^*(t)$, $I^*(t)$. Here, $r = 0.62117, K = 85, \alpha = 37, \beta = 2, \mu = 0.6, \overline{\sigma} = 0.9$.

For the improved model (5.1), in the transient dynamic process, with $\omega = 0$, $\sigma = 0$ under optimal control, which in practice can be considered as a forest area without fire, the overall tree cover in the presence of disease is lower than the tree cover in a forest area with low frequency fires ($\omega = 0.054879880$). This region has a higher I^*. When $\omega = 0.9$, grass cover was higher and fire frequency peaked, limiting the rate of disease spread. Overall tree cover at this time was higher than in diseased woodlands ($\omega = 0.$)

Fire data from some provinces in China are used next. (Shanghai, Jilin, Inner Mongolia, etc.). With these data, parameter values were obtained for several provinces from 2002 to 2018 and are shown in Table 1 (some of the data are given in Table 1), to see more clearly the trends in biomass.

Table 1. Annual forest standing tree biomass data for forest fires in each province (unit: m^3/ha).

Year	2002	2003	2008	2013	2018
Shanghai	10.97706	17.5873	16.9095	27.3642	50.5157
Inner Mongoria	66.5583	53.7157	49.7467	54.0739	58.3988
Yunnan	99.7149	89.69645	85.4803	88.4495	93.6613
Hebei	17.6961	19.7972	20.0179	24.5259	27.3289
Jilin	111.2575	113.3776	114.6019	120.7763	129.0606
Jiangsu	18.7235	32.5714	39.9136	39.9136	45.1598

According to the data in Table 1, Figure 8 shows the biomass loss under different fire frequencies in the same year. Figure 9 shows the survival of tree biomass over time under different fire frequencies.

The model is fitted to the actual data, and the results show that the model can predict to some extent the change of forest live wood volume in the next 30 years when the fire frequency is relatively stable, see Figure 10. In 2020, forest tree biomass in Jilin Province reached $138.37m^3/ha$, and through the model, we predicted that Jilin's tree biomass in 2020 would be $132.395m^3/ha$, which illustrates the reasonableness of the model.

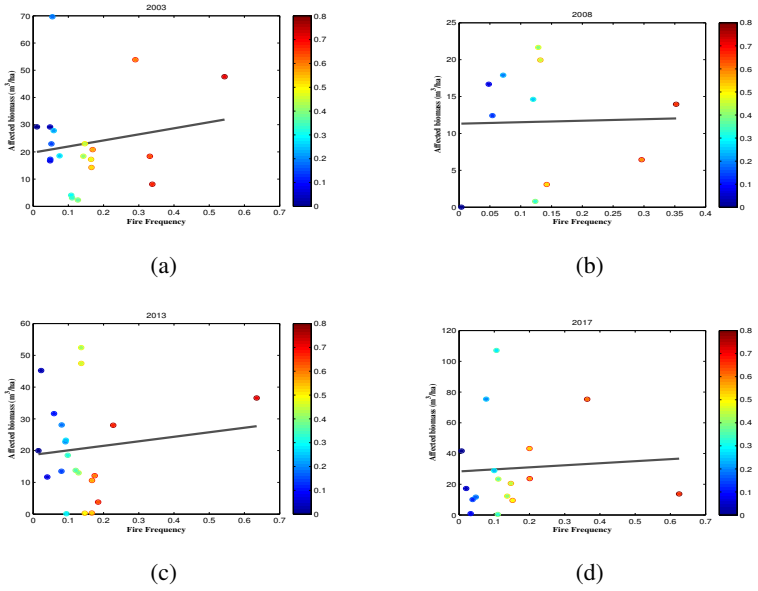

Figure 8. Trends in live forest tree biomass over time at different fire frequencies, with the number of fires per year as units on the x-axis. The grey lines are linear regressions performed within each survey year. Colors represent fire frequency groupings.

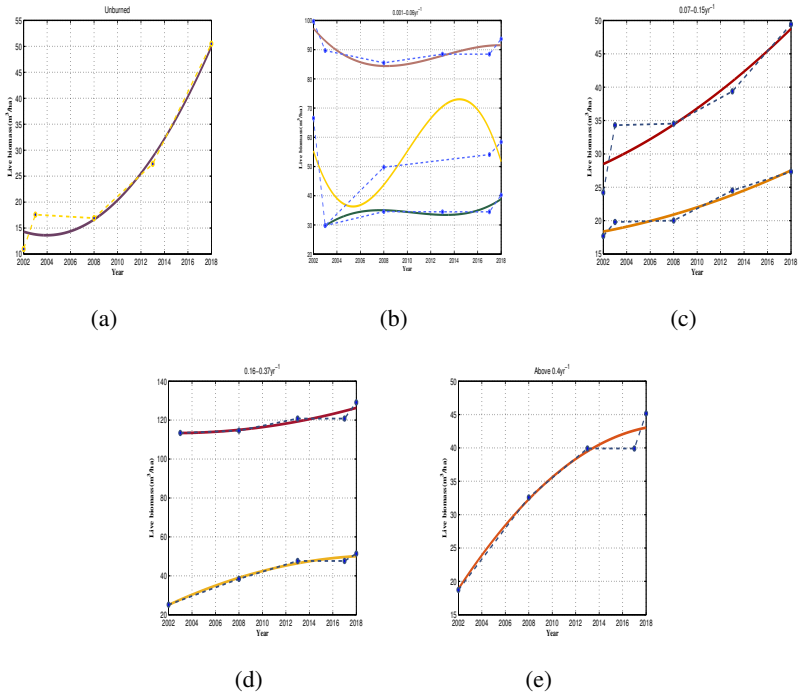

Figure 9. Longitudinal trends within the plots in the different treatments with respect to fire frequency. Raw data is expressed as points and the solid smoothed line is a generalized additive model fit within the plot. (a) Number of forests in Shanghai. (b) In order, number of forests in Yunnan, Inner Mongoria and Shanxi. (c) In order, number of forests in Guangdong and Hebei. (d) In order, number of forests in Jilin and Henan. (e) Number of forests in Jangsu.

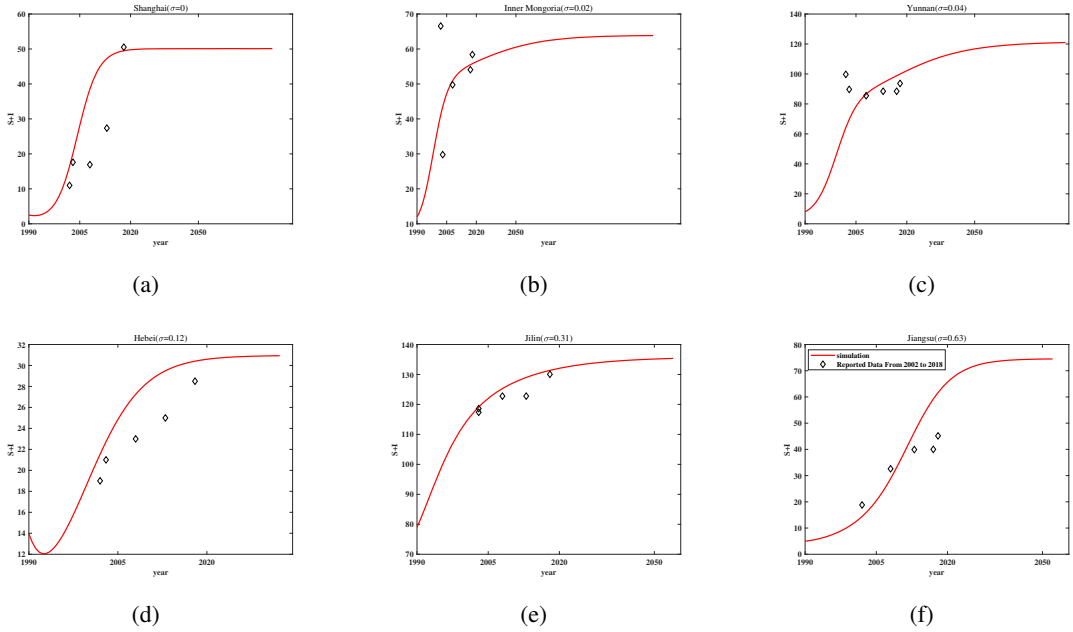

Figure 10. Predicted tendency of forest fire in Shanghai, Inner Mongolia, Yunnan, Hebei, Jilin, etc. (**a**) Number of forests in Shanghai. (**b**) Number of forests in Inner Mongoria. (**c**) Number of forests in Yunnan. (**d**) Number of forests in Hebei. (**e**) Number of forests in Jilin. (**f**) Number of forests in Jiangsu. See Table 1 for specific data.

5.2. Sensitivity analysis

Sensitivity analysis is the most commonly used test in the process of model optimization. Usually, only parameters with large uncertainties can be selected for sensitivity analysis without the need to calculate sensitivity coefficients for each parameter. A study is carried out to analyze the influence of the key parameter σ in the sensitivity characterization in order to better understand the effects of fire on forests. The specific steps of the algorithm of the coefficient of sensitivity are follows [28]. We consider the function $\dot{y(t)} = f(t, y, m)$, and the absolute sensitivity of variable y_i to parameter M:

$$P_i(t) = \frac{\partial y_i(t.M)}{\partial M}, i = 1, 2.$$

We denote the relative sensitivity of a variable to a parameter

$$p_i(t) = \frac{\partial y_i(t.M)}{\partial M}\frac{M}{y_i}, i = 1, 2$$

and the absolute sensitivity equation of parameter P_i

$$\dot{P}_i = \frac{\partial f}{\partial y}P_i + \frac{\partial f}{\partial m}, i = 1, 2.$$

According to the steps of sensitivity analysis, the sensitivity analysis and relative sensitivity analysis

are developed for the system, and then the sensitivity equation of the system contains 4 equations:

$$\begin{cases} \dot{S} = rS(1-\frac{S}{K}) - \frac{\beta}{I+\alpha}SI - \sigma\frac{S}{\omega S+1}, \\ \dot{I} = \frac{\beta}{I+\alpha}SI - \mu_1 I - \sigma I, \\ \dot{P}_1 = P_1(r - \frac{2rS}{k} - \frac{\beta I}{I+\alpha} - \frac{\sigma}{(\omega S+1}})^2) - P_2\frac{S\beta\alpha}{(I+\alpha)^2} - \frac{S}{\omega S+1}, \\ \dot{P}_2 = P_1\frac{\beta I}{I+\alpha} + P_2(\frac{S\beta\alpha}{(I+\alpha)^2} - \mu_1) - I. \end{cases} \tag{5.5}$$

Assuming the values of time step $\triangle t = 2000$ and fire frequency $\sigma = 0.6037$, the initial values are chosen to be consistent with Section 3, and the sensitivity analysis of σ on susceptible and infected trees was been carried out using the Runge-Kutta integration method of 4 (RK-4) for system (5.1), computed in the MATLAB R2021a environment. The conclusions obtained are able to reflect the degree of influence of σ on each component (susceptible and infected trees) in the forest, as shown in Figure 11.

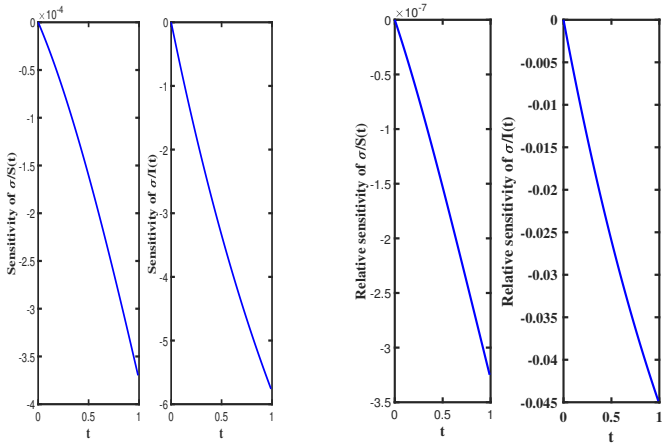

(a) (b)

Figure 11. Relative sensitivity and sensitivity of σ to S(t) and I(t).

As shown in Figure 11, the sensitivity P_1 and relative sensitivity $\sigma P_1/S(t)$ to susceptible trees $S(t)$ show a trend of less than 0. The results show a decrease in $S(t)$ with the increase of σ, and when $t = 0.5$, $P_1 = -1.606 \times 10^{-4} < 0$, $\frac{\sigma P_1}{S} = -1.531 \times 10^{-7} < 0$. That means that when σ increases by 10%, S will decrease by 1.531×10^{-6}%, and the sensitivity P_2 and relative sensitivity $\sigma P_2/I(t)$ to susceptible trees $I(t)$ show a trend of less than 0. The results show a decrease in $I(t)$ with the increase of σ, and when $t = 0.5$, $P_2 = -3.342 < 0$, $\frac{\sigma P_2}{S} = -0.026 < 0$, it means that when σ increases by 10%, I will decrease by 0.260%.

6. Discussion

We analyze the process of synergistic interaction between fire and disease in the case of tree species where fire acts on both adults and saplings. A diffusion term is added to this, where tree species may diffuse in the direction of regions rich in resources, or may diffuse in areas with few competitors because of the asymmetric competition between species, or may diffuse with the influence of external environmental factors such as water flow. Based on the above complex

ecological process, it is reasonable to describe the relationship between susceptible and infected trees by using the reaction-diffusion equation.

We present mathematical models with generalizations that provide the basis for exploring the effects of fire and insect pests on grasslands and forests. In Section 2, the disease-free equilibrium points and coexistence equilibrium points of the fire-free model are shown. The disease-free equilibrium points and coexistence equilibrium points of the disease model in the fire-free state are globally stable under certain conditions. In Section 3, we factor in fire and grassland cover in the model. Model (3.1) is developed to demonstrate the local stability of the equilibrium point of the model. The dynamical properties of the model in the case of band diffusion are discussed in Section 4. And in Section 5, we discuss the optimal control strategy for fire to find the appropriate frequency of wildfire occurrence. The results show that the biological survival in forest areas without fire but with disease is smaller than that in forest areas where fire occurs and disease is present.

Based on the forest fire data provided by the State Forestry Administration from 2002-2018, the forest development trend after fire was predicted, and the results showed that the fire factor σ plays an important role in the evolution of the forest. Further, we use sensitivity analysis to determine the degree of influence of the parameters on the model. Our empirical analysis shows that disease invasion reduces tree biomass, but that fire itself can significantly affect forest biomass in an area, which also takes into account the effect of grassland cover. Our model predictions suggest that the interaction between disease and fire in forested ecoregions jointly affects the distribution of forest ecosystems.

Use of AI tools declaration

The authors declare they have not used Artificial Intelligence (AI) tools in the creation of this article.

Acknowledgments

The authors wish to thank the editors and reviewers for their helpful comments.

Conflict of interest

The authors declare no competing interests.

References

1. N. G. Mcdowell, C. D. Allen, A. T. Kristina, Pervasive shifts in forest dynamics in a changing world, *Science*, **368** (2020), 964–976. http://dx.doi.org/10.1126/science.aaz9463
2. R. Seidl, D. Thom, M. Kautz, D. Martin-Benito, Forest disturbances under climate change, *Nat. Clim. Chang.*, **7** (2017), 395–402. http://dx.doi.org/10.1038/NCLIMATE3303
3. J. A. Hicke, C. D. Allen, A. R. Desai, Effects of biotic disturbances on forest carbon cycling in the United States and Canada, *Glob. Change Biol.*, **18** (2012), 7–34. http://dx.doi.org/10.1111/j.1365-2486.2011.02543.x

4. I. L. Boyd, P. H. Freersmith, C. A. Gilligan, H. C. J. Godfray, The consequence of tree pests and diseases for ecosystem services, *Science*, **342** (2013), 823–833. http://dx.doi.org/10.1126/science.1235773

5. A. J. Tepley, E. Thomann, T. T. Veblen, Influences of fire-vegetation feedbacks and post-fire recovery rates on forest landscape vulnerability to altered fire regimes, *J. Ecol.*, **106** (2018), 1925–1940. http://dx.doi.org/10.1111/1365-2745.12950

6. A. C. Staver, S. Archibald, S. A. Levin, The global extent and determinants of savanna and forest as alternative biome states, *Science*, **334** (2011), 230–232. http://dx.doi.org/10.1126/science.1210465

7. S. I. Higgins, W. J. Bond, W. S. W. Trollope, Fire, resprouting and variability: a recipe for grass-tree coexistence in savanna, *J. Ecol.*, **88** (2000), 213–229. http://dx.doi.org/10.1046/j.1365-2745.2000.00435.x

8. W. A. Hoffmann, E. L. Geiger, S. G. Gotsch, D. R. Rossatto, L. C. R. Silva, O. L. Lau, Ecological thresholds at the savanna forest boundary: how plant traits, resources and fire govern the distribution of tropical biomes, *Ecol. Lett.*, **15** (2012), 759–768. http://dx.doi.org/10.1111/j.1461-0248.2012.01789.x

9. D. W. Peterson, P. B. Reich, K. J. Wrage, J. Franklin, Plant functional group responses to fire frequency and tree canopy cover gradients in oak savannas and woodlands, *J. Veg. Sci.*, **18** (2007), 3–12. http://dx.doi.org/10.1111/j.1654-1103.2007.tb02510.x

10. R. K. Meentemeyer, N. J. Cunniffe, A. R. Cook, J. A. Joao, R. D. Hunter, D. M. Rizzo, Epidemiological modeling of invasion in heterogeneous landscapes: spread of sudden oak death in California (1990–2030), *Ecosphere*, **2** (2011), 1–24. http://dx.doi.org/10.1890/ES10-00192.1

11. A. Dobson, M. Crawley, Pathogens and the structure of plant communities, *Trends Ecol. Evol.*, **9** (1994), 393–398. http://dx.doi.org/10.1016/0169-5347(94)90062-0

12. R. M. Anderson, R. May, *Infectious Diseases of Humans: Dynamics and Control*, Oxford: Oxford University Press, 1991. http://dx.doi.org/10.1002/hep.1840150131

13. J. J. Burdon, G. A. Chilvers, Host density as a factor in plant disease ecology, *Annu. Rev. Phytopathol*, **20** (1982), 143–166. http://dx.doi.org/10.1146/annurev.py.20.090182.001043

14. L. S. Comita, S. A. Queenborough, S. J. Murphy, Testing predictions of the Janzen-Connell hypothesis: a meta-analysis of experimental evidence for distance-and density-dependent seed and seedling survival, *J. Ecol.*, **102** (2014), 845–856. http://dx.doi.org/10.1111/1365-2745.12232

15. J. P. Gerlach, P. B. Reich, K. Puettmann, T. Baker, Species, diversity, and density affect tree seedling mortality from Armillaria root rot, *Can. J. For. Res.*, **27** (1997), 1509–1512. http://dx.doi.org/10.1139/x97-098

16. D. W. Peterson, P. B. Reich, Prescribed fire in oak savanna: fire frequency effects on stand structure and dynamics, *Ecol. Appl.*, **11** (2001), 914–927. http://dx.doi.org/10.1890/1051-0761(2001)011[0914:PFIOSF]2.0.CO;2

17. L. E. Frelich, P. B. Reich, D. W. Peterson, *Fire in Upper Midwestern Oak Forest Ecosystems: An Oak Forest Restoration and Management Handbook*, Portland: Pacific Northwest Research Station, 2015. http://dx.doi.org/10.2737/PNW-GTR-914

18. A. F. A. Pellegrini, A. M. Hein, J. Cavender-Bares, R. A. Montgomery, Disease and fire interact to influence transitions between savanna-forest ecosystems over a multi-decadal experiment, *Ecol. Lett.*, **24** (2021), 1007–1017. http://dx.doi.org/10.1111/ele.13719
19. P. Magal, Z. Y. Zhang, A system of state-dependent delay differential equation modelling forest growth II: Boundedness of solutions, *Nonlinear Anal. Real World Appl.*, **42** (2018), 334–352. http://dx.doi.org/10.1016/j.nonrwa.2018.01.002
20. P. Magal, Z. Y. Zhang, A system of state-dependent delay differential equation modeling forest growth I: semiflow properties, *J. Evol. Equ.*, **18** (2018), 1853–1888. http://dx.doi.org/10.1007/s00028-018-0464-0
21. P. Magal, Z. Y. Zhang, Numerical simulations of a population dynamic model describing parasite destruction in a wild type pine forest, *Ecol. Complex.*, **34** (2018), 147–160. http://dx.doi.org/10.1016/j.ecocom.2017.05.001
22. P. Magal, Z. Y. Zhang, Competition for light in forest population dynamics: from computer simulator to mathematical model, *J. Evol. Equ.*, **419** (2017), 290–304. http://dx.doi.org/10.1016/j.jtbi.2017.02.025
23. J. P. Tripathi, S. Tyagi, S. Abbas, Global analysis of a delayed density dependent predator-prey model with Crowley-Martin functional response, *Commun. Nonlinear Sci. Numer. Simul.*, **30** (2015), 45–69. http://dx.doi.org/10.1016/j.cnsns.2015.06.008
24. H. Chen, C. Zhang, Dynamic analysis of a Leslie Gower type predator prey system with the fear effect and ratio-dependent Holling III functional response, *Nonlinear Anal. Model Control*, **27** (2022), 904–926. http://dx.doi.org/10.15388/namc.2022.27.27932
25. X. M. Rong, M. Fan, H. P. Zhu, Dynamic modeling and optimal control of cystic echinococcosis, *Infect. Dis. Poverty*, **10** (2021), 38. http://dx.doi.org/10.1186/s40249-021-00807-6
26. L. H. Zhou, M. Fan, Q. Hou, Z. Jin, X. D. Sun, Transmission dynamics and optimal control of brucellosis in Inner Mongolia of China, *Math. Biosci. Eng.*, **15** (2018), 543–567. http://dx.doi.org/10.3934/mbe.2018025
27. R. H. Martin, Logarithmic norms and projections applied to linear differential systems, *J. Math. Anal. Appl.*, **45** (1974), 432–454. http://dx.doi.org/10.1016/0022-247X(74)90084-5
28. X. X. Liu, C. R. Zhang, Stability and optimal control of Tree-Insect Model under forest fire disturbance, *Mathematics*, **10** (2022), 2563. http://dx.doi.org/10.3390/math10152563

AIMS Press